Asian Journal of Scientific Research

ISSN 1992-1454

science alert
http://www.scialert.net

ANSInet
an open access publisher
http://ansinet.com

OPEN ACCESS Asian Journal of Scientific Research

ISSN 1992-1454
DOI: 10.3923/ajsr.2020.92.110

Research Article
In silico Structural Modelling and Comparative Analysis of β-mannanases from Psychrophilic and Mesophilic *Arthrobacter* sp.

Wan Nur Shuhaida Wan Mahadi, Clemente Michael Wong Vui Ling, Kenneth Francis Rodrigues and Cahyo Budiman

Biotechnology Research Institute, Universiti Malaysia Sabah, Jalan UMS, 88400 Kota Kinabalu, Sabah, Malaysia

Abstract

Background and Objective: Endo-1,4-β-mannanase (β-mannanase, EC 3.2.1.78) is an industrially important enzyme which catalyses the hydrolysis of mannan-based polysaccharides. This enzyme is produced by psychrophilic and mesophilic groups of *Arthrobacter* sp., yet none of them were structurally characterized. This study aims to decipher the structural features of *Arthrobacter* β-mannanases that might responsible for their cold adaptation. **Material and Methods:** Thirty amino acid sequences encoding β-mannanases from *Arthrobacter* sp. were retrieved from GenBank and subjected to series of analysis of amino acid profiling and structural homology modelling using Phyre2 and SWISS-MODEL. **Results:** Structural alignment showed the catalytic residues (2 glutamic acids) were conserved among β-mannanase suggesting that they might shares catalytic mechanism. Psychrophilic β-mannanases showed remarkable differences from the mesophilic ones in the content of hydrophilic, particularly negatively charged, residues and proline, which were thought to be important for its cold adaptation. Three-dimensional model of all *Arthrobacter* β-mannanases forms a classic α/β barrel motif consisting of 8 helices and 9 β-sheets structures, except for psychrophilic ones, which having 8 helices and 8 β-sheets. **Conclusion:** Adaptation of *Arthrobacter* β-mannanases towards cold temperature involves structural adjustment particularly on structural flexibility and amino acid distribution.

Key words: β-mannanase, mannan, *Arthrobacter* sp., structural modelling, cold-adaptation

Citation: Wan Nur Shuhaida Wan Mahadi, Clemente Michael Wong Vui Ling, Kenneth Francis Rodrigues and Cahyo Budiman, 2020. *In silico* structural modelling and comparative analysis of β-mannanases from psychrophilic and mesophilic *Arthrobacter* sp. Asian J. Sci. Res., 13: 92-110.

Corresponding Author: Cahyo Budiman, Biotechnology Research Institute, Universiti Malaysia Sabah, Jalan UMS, 88400 Kota Kinabalu, Sabah, Malaysia Tel/Fax: +608832000

Competing Interest: The authors have declared that no competing interest exists.

Data Availability: All relevant data are within the paper and its supporting information files.

INTRODUCTION

β-mannanase or specifically endo-1,4-β-mannanase (EC 3.2.1.78) is an enzyme belonging to the glycosyl hydrolase (GH) families that catalyses the hydrolysis of β-D-1,4-mannosidic linkages in mannan based polysaccharides, leaving shorter chains of oligosaccharides[1-3]. These enzymes offer many applications, has many demands in various industries and is produced by many microorganisms in extracellular forms[3,4]. *Arthrobacter* sp. is one of the bacterial species known to produce β-mannanases and is widely found in soil and extreme contaminated environments including the Antarctic region[5-8]. This group has been found to have a growing temperature of 0-45 °C which makes this bacteria to be either categorised as psychrophilic or mesophilic group[9,10]. GenBank houses at least 30 amino acid sequences of β-mannanases from *Arthrobacter* sp. which have been isolated from psychrophilic and moderate mesophilic *Arthobacter* sp. Nevertheless, to our knowledge, none of β-mannanases of *Arthrobacter* sp. has been structurally studied extensively so far. While a number β-mannanases structures were deposited in protein data bank (PDB), none of them originated from *Arthobacter* sp. In addition, there are no inclusive reports on psychrophilic β-mannanases from any organism.

Structural studies of psychrophilic enzymes gain wide interest as the mechanisms by which the enzymes adapt to low temperature are diverse. Particularly, the cold adaptation mechanism of psychrophilic β-mannanases remains poorly understood. X-ray crystallography and nuclear magnetic resonance (NMR) spectroscopy are undoubtedly powerful tools to decipher the protein structures at atomic level. However, the technologies are costly and tedious[11,12]. On the other hand, it is important to note that amino acid sequence of proteins dictate the structural properties of the protein[13]. Furthermore, the amino acid sequence stores the information required for the determination and characterization of a protein molecule's functions, physical and chemical properties[14]. Accordingly, harnessing the amino acid sequence through a series of various platforms of computational biology (*in silico*) analysis is considerably a viable tool as an alternative over other costly technologies. *In silico* structural analysis, structural homology modelling is known to be getting more popular within this decade. This is due to the sigmoidal growth of deposited experimental data in the protein data bank (PDB) and a rapid progress of computation technology. The availability of experimental data at PDB provides various structural templates for the structural modelling with better accuracy[15].

In this study, structural features of *Arthobacter* β-mannanases isolated from various environments were analysed using various *in silico* platforms. This involves amino acid composition, chemical properties and three-dimensional structural models of these β-mannanases. The comparative analysis between mesophilic and psychrophilic *Arthobacter* β-mannanases was then used as a basis to discuss the cold adaptation mechanism of this enzyme.

MATERIALS AND METHODS

Sequence and structural retrieval: The amino acid sequences of 30 mannan endo-1,4-β-mannosidase (β-mannanase) protein was retrieved from the GenBank (https://www.ncbi.nlm.nih.gov/genbank/). The study was conducted at Biotechnology Research Institute, Universiti Malaysia Sabah, Malaysia, for the period of October, 2018-March, 2019. For comparison, previously reported β-mannanases were included in this study including CfMan26A (*Cellulomonas fimi*), MeMan5A (*Mytilus edulis*) and TrMan5A (*Trichoderma reesei*). The complete list of organisms used in this study is shown in Table 1.

The POWER web interface (http://power.nhri.org.tw/) was connected for phylogenetic tree development and investigation in light of the Dayhoff-PAM method using the amino acid sequence of the proteins[16]. The Kitsch (http://caps.ncbs.res.in/iws/phylip_files/kitsch.html) program (Fitch-Margoliash slightest squares strategy) was utilized for investigation of phylogenetic tree[17]. The unwavering quality of the assessed trees was assessed by using the Bootstrap strategy with 1000 replications.

Primary structural analysis and secondary structural analysis: ExPasy (Expert Protein Analysis System) ProtParam server[18] has been 100 utilized for physiochemical characterization of the β-mannanases. These parameters include theoretical isoelectric points (pI), molecular weights, the total number of positive and negative residues, instability index, aliphatic index and the grand average hydropathy (GRAVY)[19-21]. PSIPRED was used for secondary structure analysis of the proteins[22]. It is a server that uses the principle of 2 feeds which are the forward and neural networks.

Analysis of conserved catalytic residues: Analysis of the sequences was conducted using Clustal Omega-MSA for obtaining pairwise distance[23,24]. The catalytic residues of the β-mannanases were determined using sequence alignment

Table 1: List of *Arthobacter* strains producing β-mannanases used in this study

Strains	Codes	Accession numbers (GenBank)	Growing temperature (°C)/type	References
135MFCol5.1	A1	WP_018762220.1	N/A	
162MFSha1.1	A2	WP_026265823.1	N/A	
31Cvi3.1E	A3	SKB67575.1	N/A	
49Tsu3.1M3	A4	SKB72436.1	N/A	
Agilis	A5	WP_087028622.1	20-30/Mesophile	JGI
Br18	A6	WP_052274099.1	15/Psychrophile	JGI
Enclensis	A7	KSU78669.1	30/Mesophile	Dastager *et al*.,
EPSL27	A8	KUM33307.1	N/A	
FB24	A9	WP_043430353.1	Mesophile	JGI
Globiformis	A10	WP_003803021.1	Psychrophilic	Berger *et al*.,
L77	A11	WP_052274099.1	Psychrophile	Singh *et al*.,
Leaf137	A12	WP_056075972.1	Mesophile	JGI
Leaf141	A13	WP_056596147.1	N/A	
Leaf234	A14	WP_055769075.1	Mesophile	JGI
Leaf337	A15	WP_055797900.1	Mesophile	JGI
Luteus	A16	AQQ16388.1	N/A	
Nitrophenolicus	A17	ELT45426.1	30/Mesophile	Arora and Jain
OV608	A18	WP_091416456.1	N/A	
OY3WO11	A19	WP_066280927.1	22/Mesophile	Town *et al*.,
P2b	A20	WP_079596712.1	N/A	
Pseudarthrobacter chlorophenolicus	A21	WP_015938113.1	Mesophile	JGI
Pseudarthrobacter phenanthrenivorans	A22	WP_052259887.1	30/Mesophile	JGI
Pseudarthrobacter sulfonivorans	A23	WP_058932997.1	Psychrophilic	Zhang *et al*.,
RIT-PI-e	A24	WP_049830849.1	Mesophile	Tran *et al*.,
Soil761	A25	KRE76147.1	Mesophile	JGI
Soil764	A26	WP_056329268.1	Mesophile	JGI
SPG23	A27	WP_043479121.1	Mesophile	Gkorezis *et al*.,
U41	A28	WP_069949883.1	N/A	
UNC362MFTsu5.1	A29	WP_043439180.1	Mesophile	JGI
ZBGIO	A30	WP_050683930.1	Mesophile	JGI

from 3 reported and well-studied β-mannanases from *Cellulomonas fimi*, *Mytilus edulis* and *Trichoderma reesei*. The active sites of those β-mannanases (E175/E282, E177/E308 and E169/E276, for *Cellulomonas fimi*, *Mytilus edulis* and *Trichoderma reesei*, respectively) were used as references[25-27].

Homology protein modelling: The modelling of the 3D structure of the β-mannanases was performed using SWISS-MODEL and Phyre2 servers[28] and displayed using PyMoL software[29]. The models were then evaluated by Verify 3D (http://toolkit.tuebingen.mpg.de/modeller/verity3d/), the Ramachandran plot using RAMPAGE (mordred.bioc.cam.ac.uk/~rapper/rampage.php), GMQE (Global Model Quality Estimation) and QMEAN (the Qualitative Model Energy Analysis) scores[30]. The B-factor of each protein was calculated from the ResQ server (http://zhanglab.ccmb.med.umich.edu/)[31].

RESULTS

***Arthrobacter* producing β-mannanases:** Table 1 showed the 30 *Arthrobacter* strains producing 1,4-β-D mannanase from various environments including soil, water and plants. Based on their growth temperatures, 4 strains were identified as psychrophilic bacteria while 16 strains were classified as mesophilic bacteria. In addition, the optimum growth temperatures for the rest of 10 strains are unknown. Phylogenetic analysis of the thirty β-mannanases and 3 of the control was shown in Fig. 1. The distance between *Arthrobacter* β-mannanases were relatively close to each other, exceptionally with the three controls and A16 which is a slightly different species as mentioned previously.

Primary structure profile: Primary structure analysis showed that all β-mannanases from these bacteria were multi-domain proteins with a catalytic domain as a structural region responsible for the catalytic activity (Fig. 2). Amino acid sequences of these β-mannanases were found to have low similarities to the well-studied β-mannanases: TriMan5A, CFMan26, MeMAN5A (Table 2). Interestingly, the similarities among *Arthrobacter* β-mannanases also varied from 17.67-87.95%. Further analysis of the amino acid sequences shown in Fig. 3 revealed that the theoretical sizes and isoelectric point (pI) of the full-length were higher than the catalytic domain. Further, the instability index values, the aliphatic index and the grand average of hydrophobicity

(GRAVY) of the full-length of *Arthrobacter* β-mannanases were also remarkably higher than that of the catalytic domain.

Amino acid profile: Figure 4 revealed that the full-length of *Arthrobacter* β-mannanases were dominated by hydrophobic residues followed by neutral, hydrophilic, charged and pro residues. Similar patterns were also found in the catalytic domain. Nevertheless, the hydrophilic residues were found to be higher than the neutral residues. Overall, the full-length had remarkable higher hydrophobic, neutral and proline

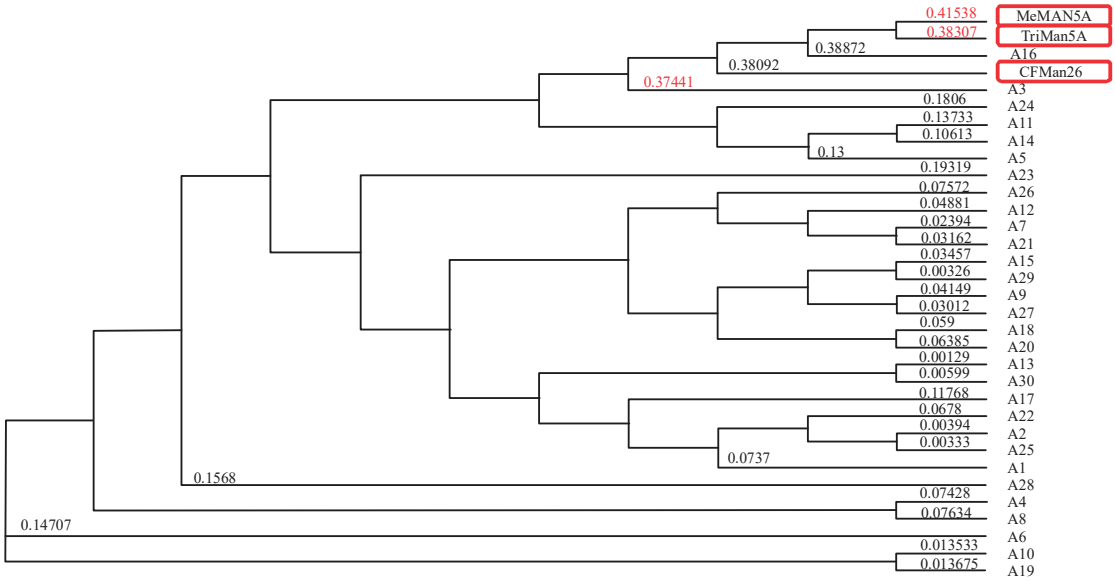

Fig. 1: Phylogenetic tree analysis among *Arthrobacter* β-mannanases and 3 controls (highlighted in red boxes)

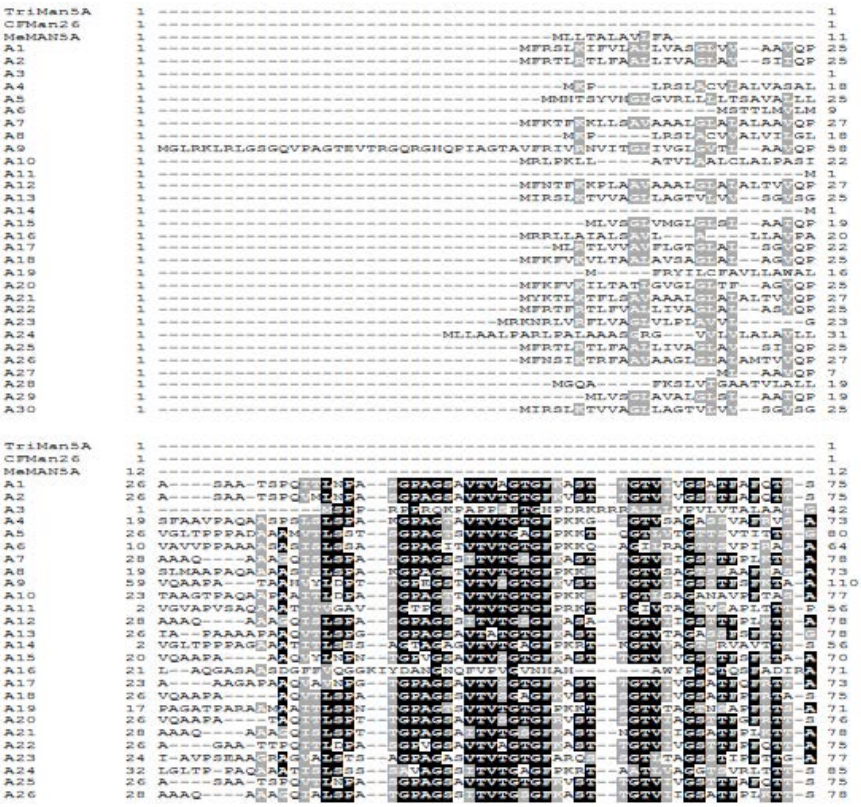

Fig. 2: Continue

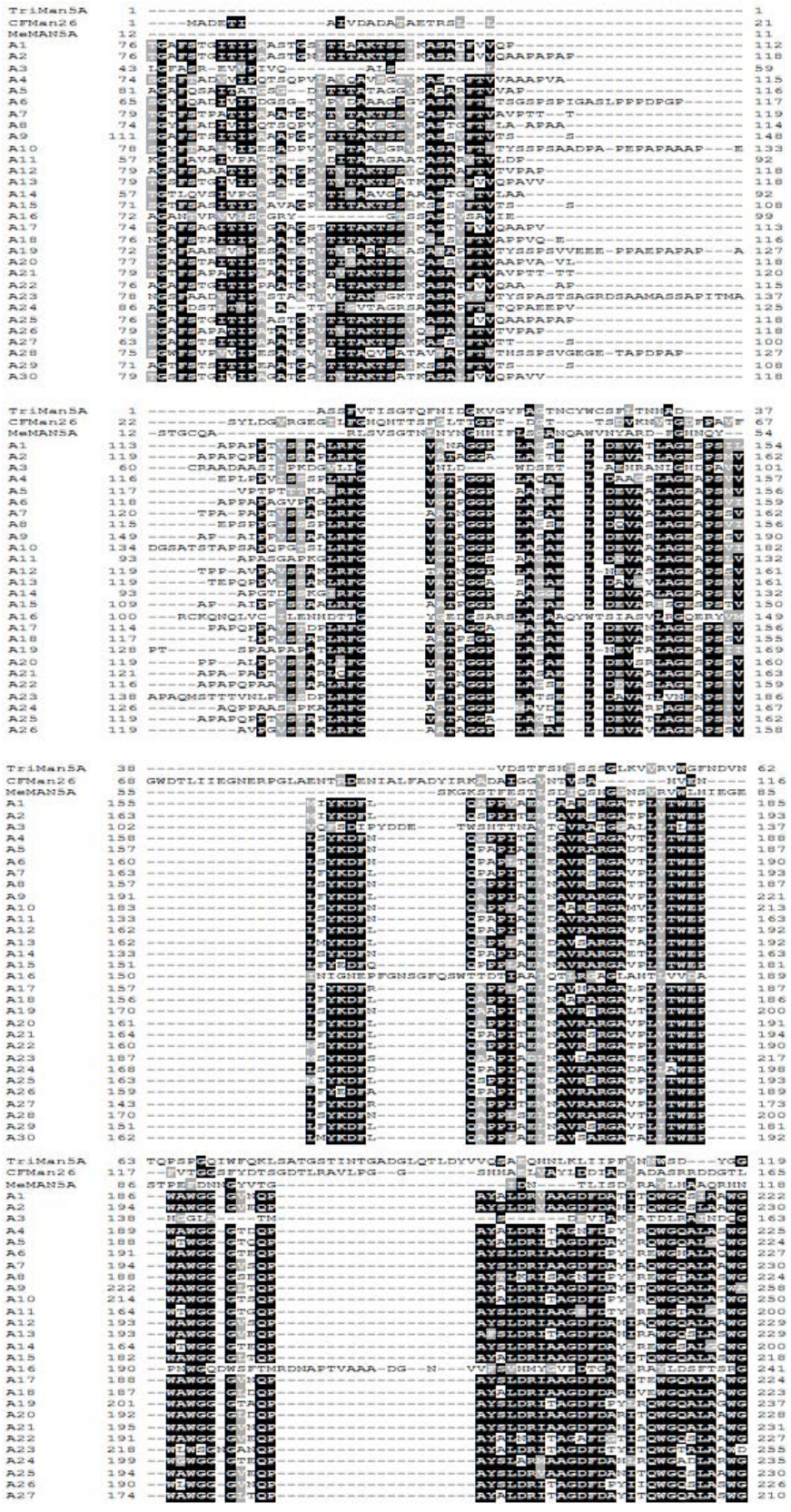

Fig. 2: Continue

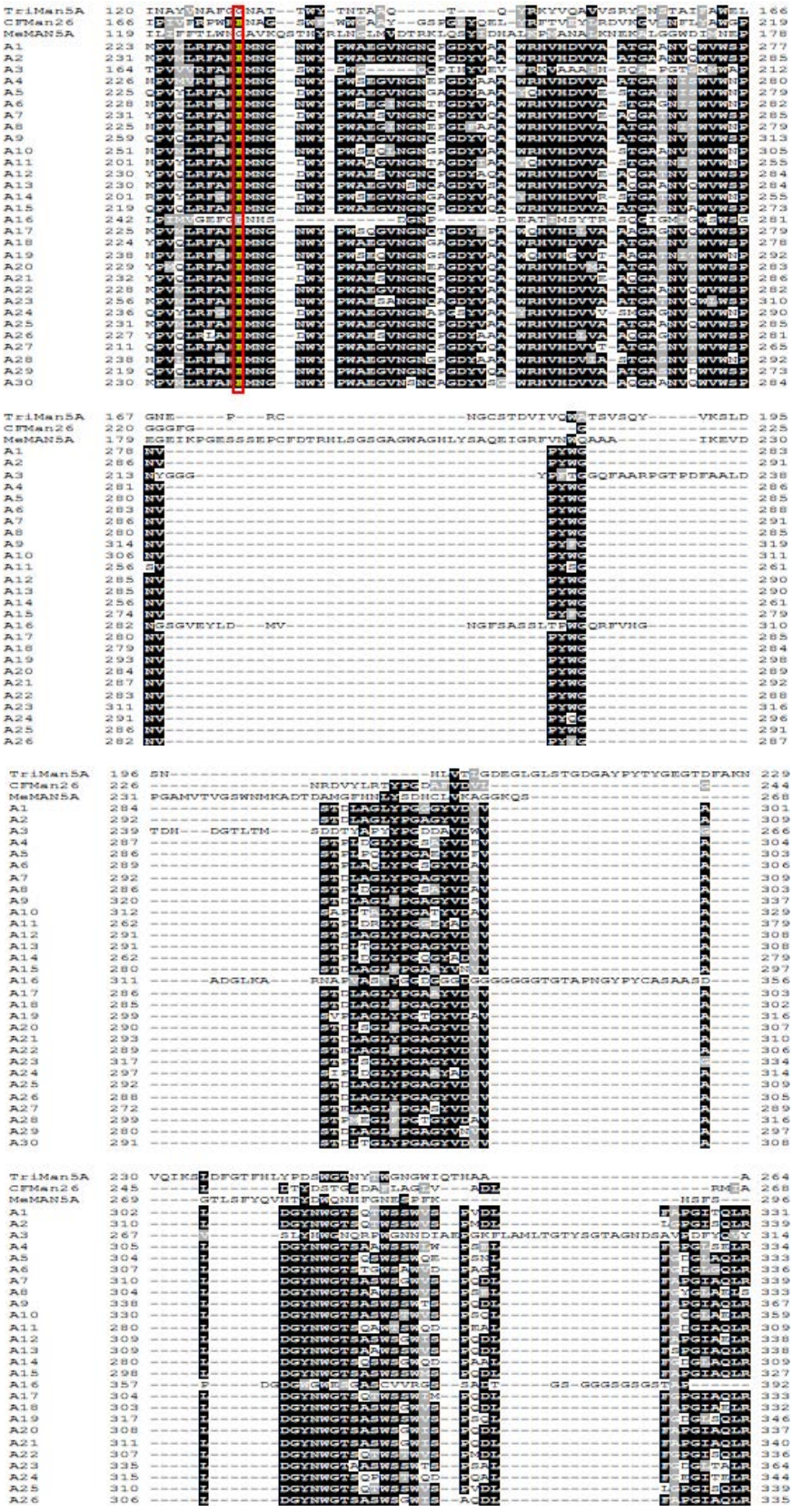

Fig. 2: Continue

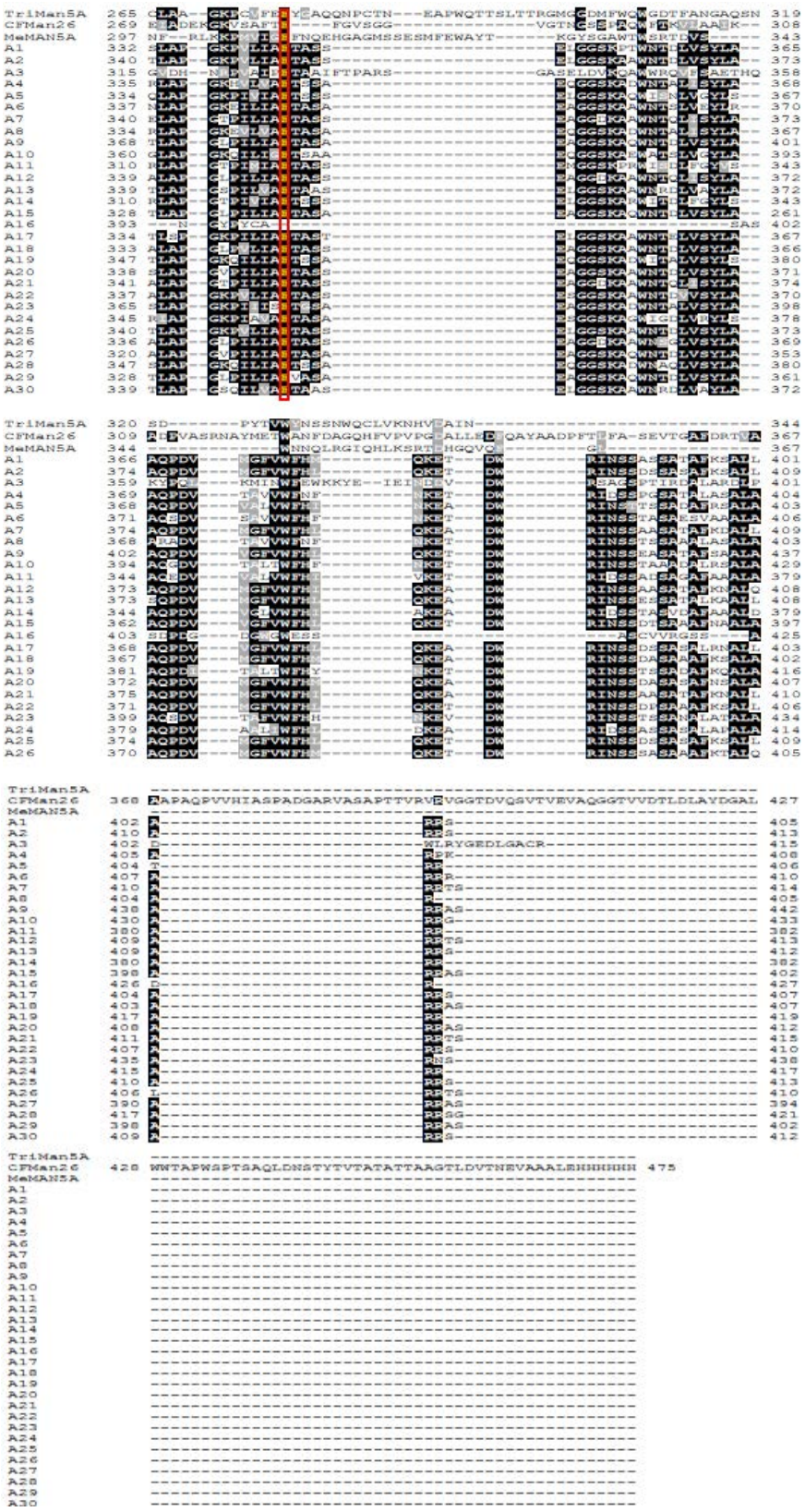

Fig. 2: Multiple sequence alignment among *Arthrobacter* β-mannanases

Table 2: Amino acid percent identity of *Arthobacter* β-mannanases

Strains	TriM	CfM	MeM	A1	A2	A3	A4	A5	A6	A7	A8	A9	A10	A11	A12	A13	A14
TriMan5A	100.00																
CfMan26A	21.55	100.00															
MeMan5A	20.16	14.04	100.00														
A1	16.75	22.65	13.42	100.00													
A2	17.22	23.00	14.59	87.16	100.00												
A3	13.78	23.10	16.39	25.45	26.51	100.00											
A4	16.75	24.39	13.78	61.36	62.09	25.45	100.00										
A5	17.70	23.16	12.99	58.29	60.15	24.46	61.65	100.00									
A6	16.27	23.00	14.55	60.88	61.48	26.67	68.34	64.87	100.00								
A7	15.79	22.65	12.45	74.31	75.43	27.71	60.35	60.20	63.52	100.00							
A8	16.27	24.56	12.00	61.17	61.81	24.39	84.94	61.21	71.14	59.80	100.00						
A9	14.83	23.69	11.16	74.81	75.25	25.08	61.62	62.00	62.53	76.66	60.41	100.00					
A10	15.79	22.65	12.93	58.75	57.84	25.83	69.12	63.84	71.39	60.05	70.86	59.80	100.00				
A11	16.27	22.81	12.27	57.98	58.09	25.08	60.21	71.47	65.18	58.99	61.84	59.79	58.90	100.00			
A12	15.31	23.00	12.88	71.32	72.91	26.51	61.10	60.45	62.66	91.28	60.55	74.63	59.46	58.73	100.00		
A13	17.22	21.60	14.22	74.81	75.79	25.98	62.44	58.71	60.71	68.8	62.16	70.79	59.21	59.47	67.57	100.00	
A14	17.70	24.91	11.36	61.17	62.07	26.30	62.83	76.44	67.80	63.76	63.16	62.17	62.83	75.65	61.90	61.32	100.00
A15	15.31	24.04	11.74	73.86	74.81	25.38	61.32	61.01	61.40	75.75	60.36	88.81	59.09	59.15	73.18	70.28	60.74
A16	20.35	17.93	13.66	20.50	19.75	17.67	22.08	17.13	20.51	21.67	19.56	20.19	20.00	18.09	21.36	22.15	19.41
A17	15.79	23.00	14.66	75.87	79.80	25.98	59.50	59.40	61.03	71.71	58.44	74.44	57.46	58.99	70.72	74.69	61.11
A18	15.31	24.48	11.69	76.63	76.37	25.00	60.45	61.06	61.24	80.69	59.90	83.13	59.85	57.71	78.47	70.47	62.50
A19	14.83	23.51	14.73	60.10	59.95	24.46	68.73	65.99	70.20	62.81	69.58	61.93	72.79	63.61	62.47	60.96	66.23
A20	15.79	24.74	11.59	74.50	74.94	25.98	60.65	62.25	60.77	78.48	59.34	82.11	57.88	59.26	76.96	69.95	64.02
A21	16.27	23.34	13.30	74.06	74.02	27.71	59.95	59.20	62.09	94.44	58.65	75.43	58.68	58.73	90.31	69.04	63.23
A22	16.75	22.30	12.02	83.70	87.32	24.70	62.06	59.15	60.93	74.07	61.52	74.50	59.51	58.89	72.52	72.48	60.48
A23	14.29	20.83	13.03	61.85	61.37	23.12	61.60	60.15	59.55	59.61	62.81	63.46	59.86	57.48	59.75	62.41	60.37
A24	16.27	23.78	11.30	55.67	56.08	25.91	56.50	67.08	62.53	58.66	56.53	56.05	59.01	65.53	58.31	56.33	70.53
A25	17.22	23.00	14.59	87.65	99.27	26.51	62.09	60.40	61.48	75.43	61.81	75.25	58.09	58.36	72.66	75.79	62.33
A26	15.31	21.95	12.99	71.25	72.46	25.23	59.00	58.46	61.28	85.12	58.94	74.26	58.17	57.94	87.32	67.90	60.32
A27	15.31	24.04	11.26	76.36	76.80	25.38	63.85	63.57	61.54	78.46	62.11	92.84	61.58	59.32	76.86	72.49	61.68
A28	15.31	23.26	13.27	59.19	58.81	27.19	68.14	63.50	66.99	59.65	66.67	63.16	68.10	62.30	61.54	61.54	65.45
A29	15.79	23.34	13.04	75.38	75.31	23.26	60.81	61.01	61.40	77.5	60.61	88.31	60.35	58.62	74.69	70.28	60.48
A30	16.75	21.60	13.79	74.07	75.06	25.68	62.19	58.21	60.46	68.06	61.90	70.30	59.21	58.95	67.08	99.27	60.79

	A15	A16	A17	A18	A19	A20	A21	A22	A23	A24	A25	A26	A27	A28	A29	A30
A15	100.00															
A16	18.73	100.00														
A17	75.44	20.56	100.00													
A18	81.36	19.24	73.87	100.00												
A19	60.56	20.77	60.51	60.15	100.00											
A20	78.86	19.94	73.07	87.71	59.95	100.00										
A21	74.75	21.67	72.95	79.26	61.15	77.80	100.00									
A22	73.30	19.14	75.50	76.25	60.66	73.58	71.92	100.00								
A23	63.64	18.10	61.29	61.60	62.14	60.34	58.97	61.33	100.00							
A24	57.80	18.58	56.28	55.78	59.95	56.61	57.53	56.00	54.32	100.00						
A25	74.81	19.75	79.80	76.62	60.20	75.18	73.77	87.32	61.37	55.83	100.00					
A26	74.06	20.94	70.57	76.98	60.71	75.62	84.88	71.32	59.70	55.97	72.46	100.00				
A27	89.23	21.22	75.97	84.42	63.33	83.85	78.21	76.80	64.18	57.77	76.80	76.23	100.00			
A28	62.03	18.87	59.35	61.65	69.81	61.69	59.26	59.75	62.23	59.70	58.81	59.95	63.52	100.00		
A29	93.28	19.05	73.42	82.87	61.58	80.10	76.25	74.81	63.38	57.54	75.31	74.06	87.95	62.53	100.00	
A30	69.77	21.85	73.96	69.98	60.96	69.46	68.3	71.74	61.92	55.83	75.06	67.41	71.98	61.54	69.77	100.00

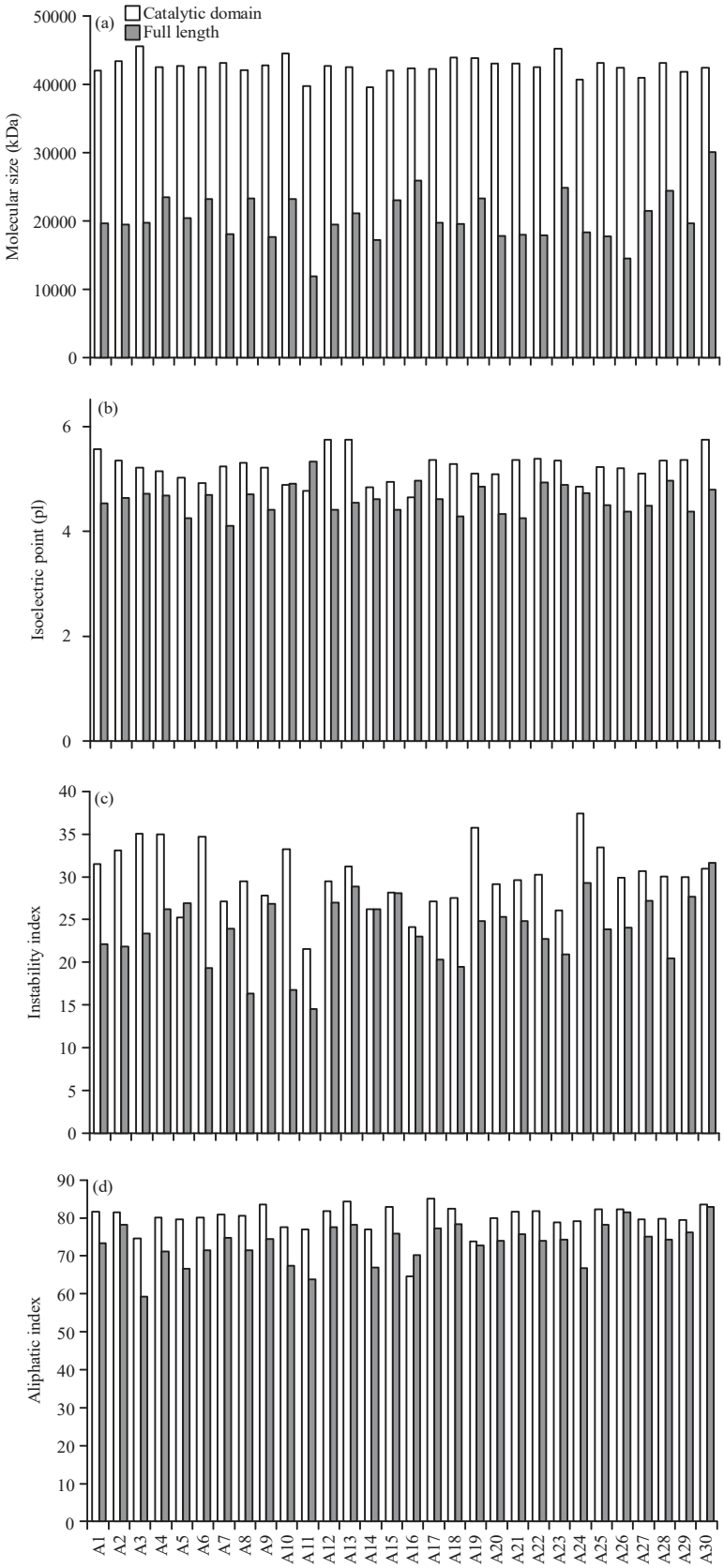

Fig. 3(a-e): Continue

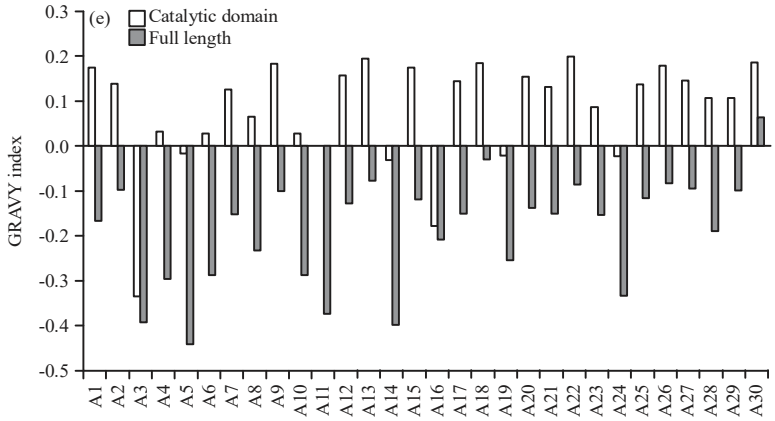

Fig. 3 (a-e): Theoretical chemical properties of *Arthrobacter* β-mannanases

Table 3: Overall comparison between amino acid profile and theoretical chemical properties of psychrophilic and mesophilic β-mannanases

	Psychrophilic (n = 4)			Mesophilic (n = 16)		
Properties	Full length	Catalytic domain	Average	Full length	Catalytic domain	Average
Hydrophobic (%)	59.30	49.48	54.390	60.16	53.42	56.790
Neutral (%)	22.18	21.85	22.015	23.41	20.59	22.000
Hydrophilic (%)	22.28	37.30	29.790	18.79	34.28	26.535
Charged (%)	13.15	13.35	13.250	11.99	12.29	12.140
Negatively charged residues (%)	7.88	8.78	8.330	6.88	8.66	7.770
Positively charged residues (%)	5.23	4.58	4.905	5.09	3.57	4.330
Proline (%)	7.43	5.35	6.390	6.79	6.58	6.685
Instability index	29.05	17.81	23.430	30.12	25.90	28.010
Aliphatic index	78.95	69.49	74.220	81.43	74.90	78.165
GRAVY	0.147	-0.272	-0.0625	0.11	-0.17	-0.030

Table 4: Predicted secondary structure comparison between psychrophilic and mesophilic *Arthrobacter* β-mannanases

	Psychrophilic (n = 4)			Mesophilic (n = 16)		
Properties (%)	Full length	Catalytic domain	Average	Full length	Catalytic domain	Average
α-helix	27.52	33.79	30.655	29.77	32.65	31.21
β-turn	6.36	8.38	7.370	6.13	7.69	6.91
Extended strand	20.22	15.15	17.685	20.06	14.94	17.50
Random coil	45.90	42.68	44.290	44.04	44.72	44.38

residues than the catalytic domain. Further, Table 3 revealed that β-mannanases from psychrophilic bacteria were found to have higher hydrophilic and charged residues than the mesophilic group. Meanwhile, neutral residues and proline of both groups were similar. Further, Table 3 also showed that hydrophilic residues of the full-length psychrophilic *Arthrobacter* β-mannanases were higher than that of the mesophilic group. By contrast, remarkable differences between the catalytic domain of β-mannanases from psychrophilic and mesophilic groups were observed in hydrophobic and hydrophilic groups (Table 3). In addition, Table 3 also showed that the instability index of mesophilic *Arthrobacter* β-mannanases was found to be higher than that of psychrophilic *Arthrobacter* β-mannanases. This was particularly observed in the catalytic domains of both β-mannanases. In addition, the aliphatic index and GRAVY of full-length and catalytic domains of mesophilic *Arthrobacter* β-mannanases were also higher than that of psychrophilic *Arthrobacter* β-mannanases.

Secondary structure profile: Figure 5 showed the full-length and catalytic domain of *Arthrobacter* β-mannanases were dominated by coil structures, followed by α-helix, β-sheet and β-turn secondary structures. Furthermore, Table 4 revealed that the full-length and catalytic domain of psychrophilic and mesophilic *Arthrobacter* β-mannanases were dominated by random coil structures, followed by α-helix, β-sheet and β-turn contents (Table 4). Among these secondary structures, only

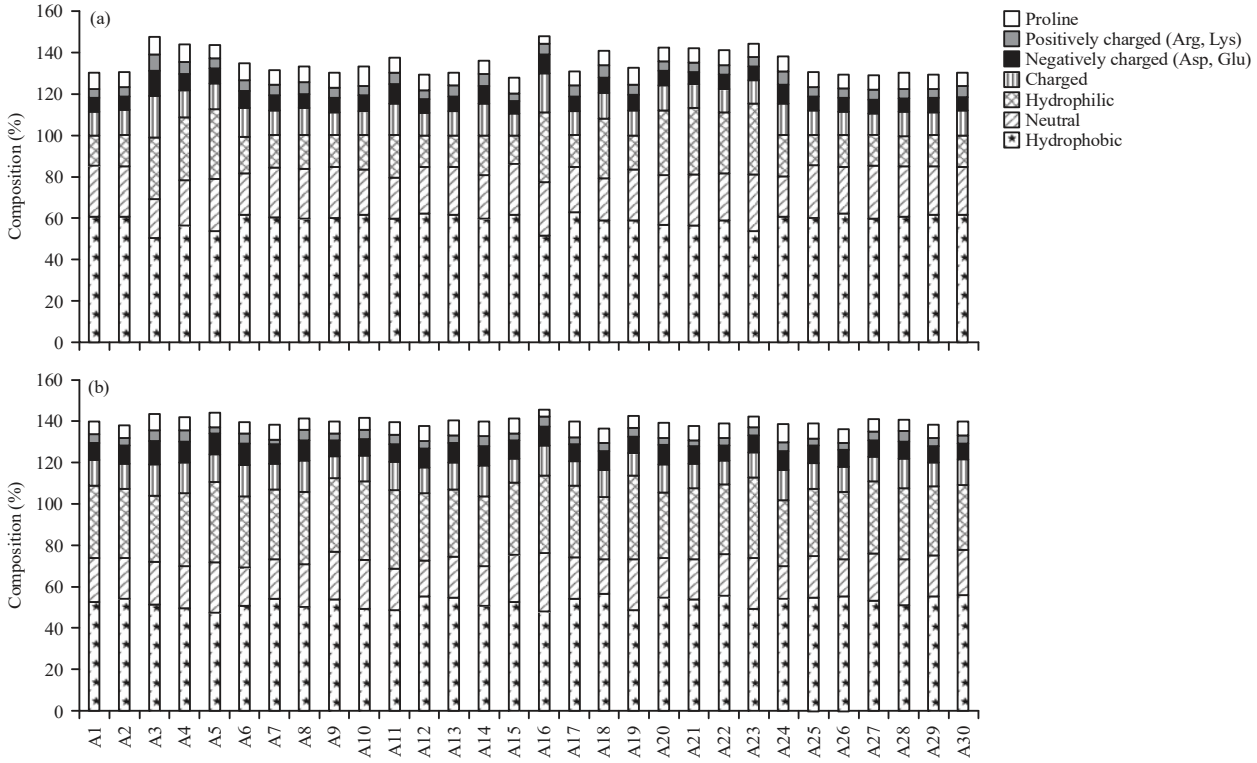

Fig. 4 (a-b): (a) Amino acid compositions of the full-length and (b) Catalytic domain of *Arthrobacter* β-mannanases

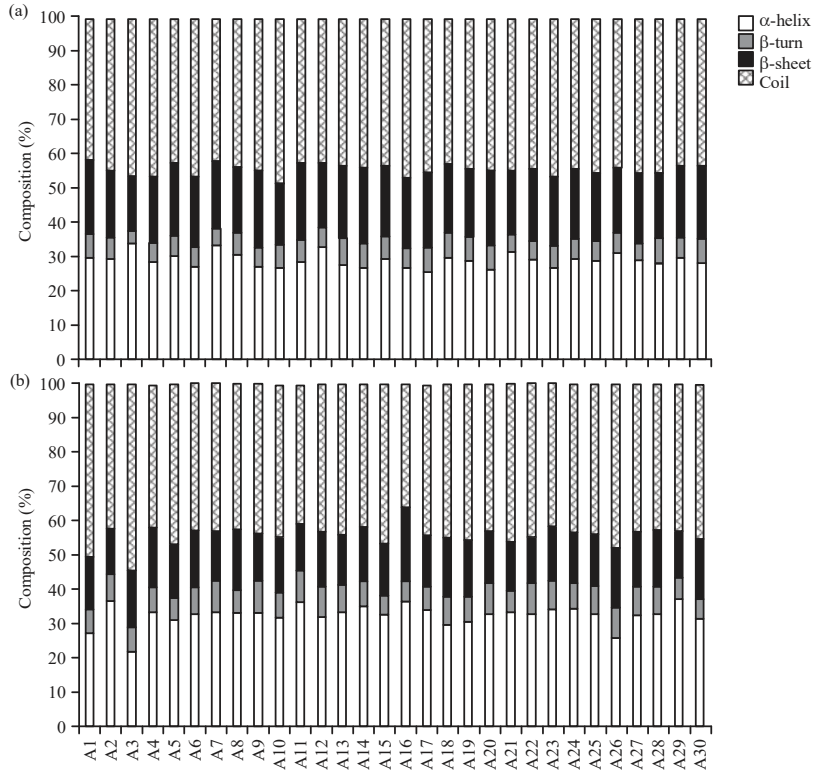

Fig. 5 (a-b): (a) Predicted secondary structure profiles of the full-length and (b) Catalytic domain of *Arthrobacter* β-mannanases

α-helix contents of the full-length psychrophilic and mesophilic *Arthrobacter* β-mannanases were found to be considerably different. Meanwhile, the catalytic domain of the psychrophilic group has lower content of random coil secondary structures than that of the mesophilic group, while the other secondary structures were considerably comparable (about 1% difference only).

Three-dimensional model structures: The 30 selected models as shown in Fig. 6 were mostly built based on the template of

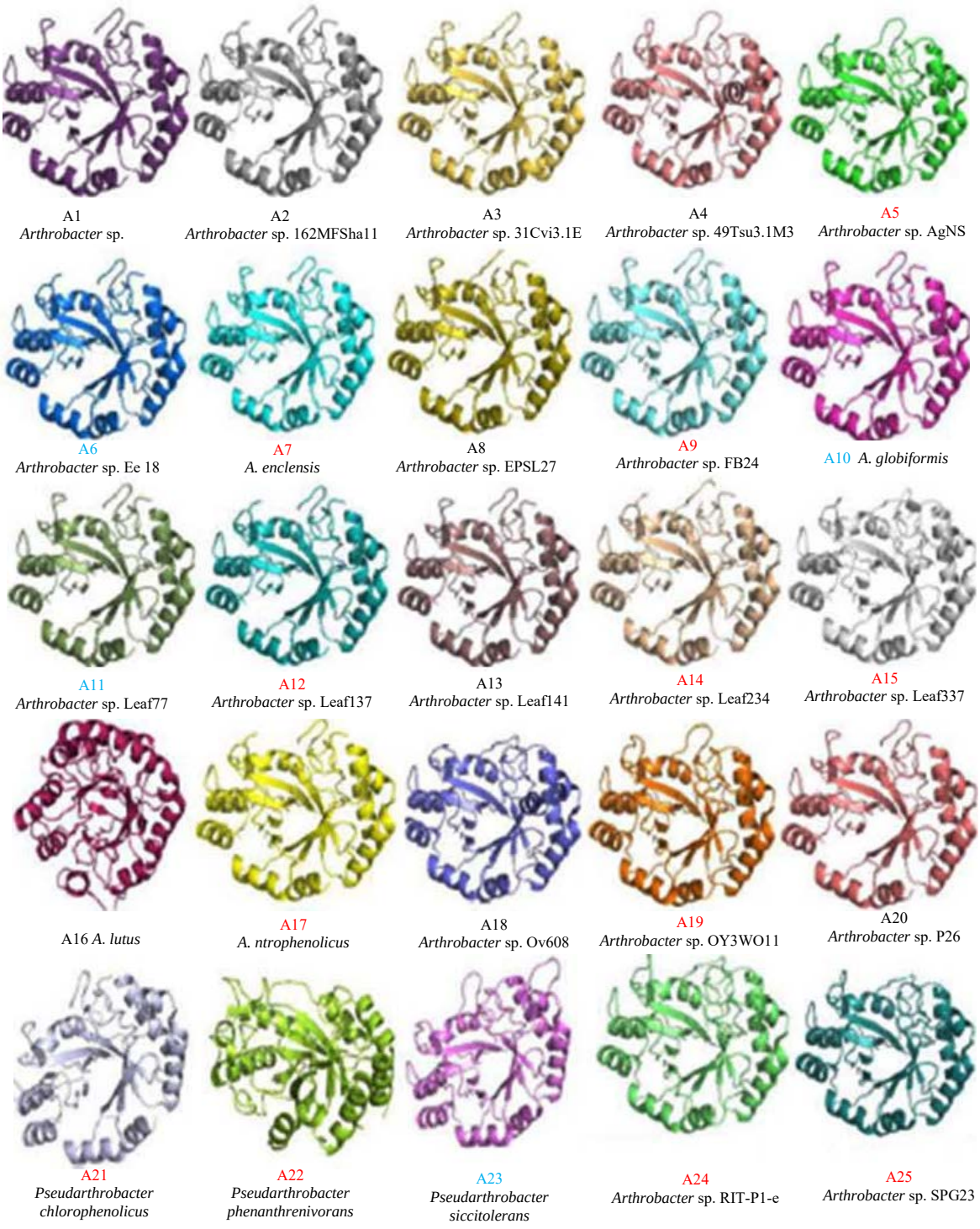

Fig. 6: Continue

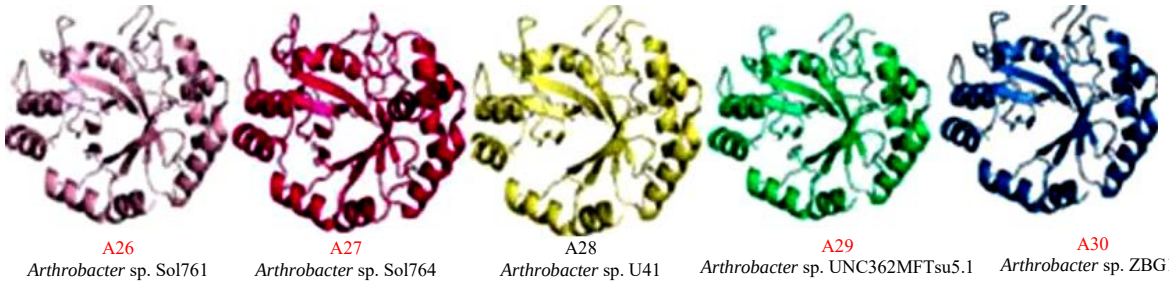

Fig. 6: Selected 3D models generated from SWISS-MODEL for *Arthrobacter* β-mannanases (designated as A1-A30 accordingly)

Black label is those originated from the strain with unknown growth temperature, red label is mesophilic β-mannanase, blue label is psychrophilic β-mannanase, all models are viewed using Pymol software

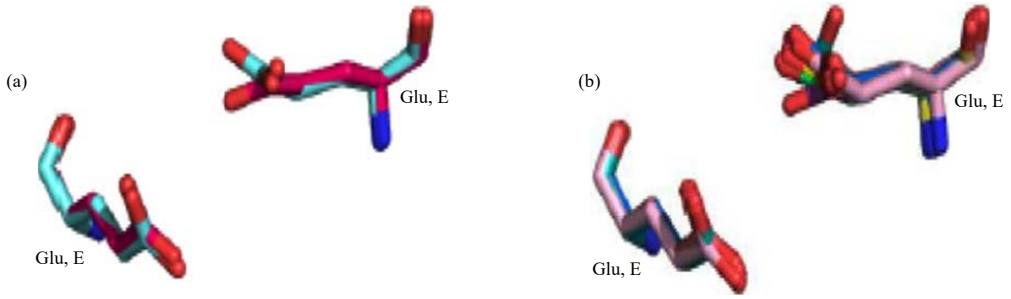

Fig. 7 (a-b): Alignment of the glutamic acids active sites among (a) Psychrophilic and (b) Mesophilic *Arthrobacter* β-mannanases

endoglucanase H of *Clostridium thermocellum* (PDB ID:2V3G) under the SCOP domain of D2V3GA1. All these models were selected as these models met the standards for structural quality parameters including structural geometry (Ramachandran plot), GCMQE, QMEAN and Verify-3D. The Ramachandran plot revealed that most of the residues of *Arthrobacter* β-mannanases were located in favoured regions (94-98%). In addition, all selected structures had GMQE scores ranging from 0.51-0.96 which were considered to be in the moderate to high score level. Meanwhile, the selected models have acceptable z-score (QMean), ranging from -4-0, which was considered a good structure model. Besides, 3D-1D score residues (Verify-3D) of all selected models were considered to be a good model as the scores were ranging from 96-100% (higher than the minimum standard of 65%). The best model selected were mostly built based on Phyre2 (19 models) and the SWISS-MODEL (11 models) platforms.

Figure 6 showed that all *Arthrobacter* β-mannanases folded into a classic $(\beta/\alpha)_8$-barrel whereby the helices and strands form a solenoid that curved around to close on itself in a doughnut shape. The parallel β-strands formed the inner wall of the doughnut (hence, a β-barrel), whereas the α-helices formed the outer wall of the doughnut. Each β-strand connected to the next adjacent strand in the barrel through a long right-handed loop that included one of the helices, so that the ribbon N-to-C colouring at the top view proceeded in rainbow order around the barrel. In general, Table 5 indicated all structures showed high similarity among each other as indicated by low RMSD values of Cα-atoms (0.00-0.036 Å), with the exception of strain A16. Comparative analysis between the models of *Arthrobacter* β-mannanases from psychrophilic and mesophilic revealed the structures were highly similar (Table 5). Furthermore, 2 active sites of glutamic acids between the psychrophilic and mesophilic β-mannanases also indicated the residues were in highly-conserved placement (Fig. 7). In addition, B-factors for the 1st and 2nd catalytic residues of the psychrophilic group ranged from 20.00-24.10 (average: 21.93) and 25.57-32.65 (average: 29.76). Meanwhile, B-factors for the 1st and 2nd catalytic residues of the mesophilic group ranged from 20.00-24.10 (average: 21.93) and 25.01-32.51 (average:30.71) (Table 6).

DISCUSSION

Primary structural analysis revealed that the size and amino acid number of the *Arthrobacter* β-mannanases are

Table 5: RMSD matrix comparison between all 3D models

Strains	A1	A2	A3	A4	A5	A6	A7	A8	A9	A10	A11	A12	A13	A14	A15
A1	0	0.000	0.000	0.260	0.105	0.000	0.000	0.000	0.000	0.000	0.000	0.000	0.000	0.000	0.111
A2		0	0.000	0.263	0.111	0.000	0.000	0.000	0.000	0.000	0.000	0.000	0.000	0.000	0.121
A3			0	0.249	0.117	0.000	0.000	0.000	0.000	0.000	0.000	0.000	0.000	0.000	0.135
A4				0	0.249	0.264	0.260	0.261	0.260	0.261	0.260	0.264	0.259	0.264	0.255
A5					0	0.111	0.115	0.115	0.106	0.115	0.115	0.111	0.106	0.115	0.065
A6						0	0.000	0.000	0.000	0.000	0.000	0.000	0.000	0.000	0.121
A7							0	0.000	0.000	0.000	0.000	0.000	0.000	0.000	0.118
A8								0	0.000	0.000	0.000	0.000	0.000	0.000	0.120
A9									0	0.000	0.000	0.000	0.000	0.000	0.110
A10										0	0.000	0.000	0.000	0.000	0.119
A11											0	0.000	0.000	0.000	0.118
A12												0	0.000	0.000	0.121
A13													0	0.000	0.111
A14														0	0.123
A15															0

	A16	A17	A18	A19	A20	A21	A22	A23	A24	A25	A26	A27	A28	A29	A30
A1	12.375	0.000	0.302	0.268	0.000	0.000	0.349	0.260	0.266	0.251	0.000	0.299	0.000	0.000	0.000
A2	12.735	0.000	0.298	0.268	0.000	0.000	0.358	0.261	0.271	0.253	0.000	0.298	0.000	0.000	0.000
A3	10.493	0.000	0.301	0.264	0.000	0.000	0.323	0.254	0.260	0.269	0.000	0.382	0.000	0.000	0.000
A4	7.670	0.264	0.113	0.052	0.260	0.260	0.349	0.081	0.089	0.071	0.259	0.104	0.261	0.261	0.260
A5	9.124	0.109	0.271	0.255	0.115	0.115	0.335	0.250	0.251	0.246	0.107	0.281	0.115	0.112	0.115
A6	7.859	0.000	0.298	0.268	0.000	0.000	0.356	0.261	0.271	0.253	0.000	0.298	0.000	0.000	0.000
A7	8.046	0.000	0.300	0.267	0.000	0.000	0.356	0.260	0.267	0.251	0.000	0.297	0.000	0.000	0.000
A8	7.941	0.000	0.298	0.268	0.000	0.000	0.374	0.261	0.269	0.251	0.000	0.298	0.000	0.000	0.000
A9	10.971	0.000	0.297	0.267	0.000	0.000	0.357	0.258	0.265	0.252	0.000	0.299	0.000	0.000	0.000
A10	6.335	0.000	0.298	0.268	0.000	0.000	0.356	0.261	0.268	0.251	0.000	0.297	0.000	0.000	0.000
A11	14.061	0.000	0.298	0.267	0.000	0.000	0.356	0.260	0.267	0.251	0.000	0.297	0.000	0.000	0.000
A12	8.419	0.000	0.298	0.268	0.000	0.000	0.356	0.261	0.271	0.253	0.000	0.298	0.000	0.000	0.000
A13	7.541	0.000	0.302	0.267	0.000	0.000	0.356	0.260	0.266	0.252	0.000	0.296	0.000	0.000	0.000
A14	11.306	0.000	0.300	0.268	0.000	0.000	0.350	0.261	0.267	0.252	0.000	0.299	0.000	0.000	0.000
A15	7.304	0.113	0.276	0.263	0.119	0.118	0.313	0.252	0.256	0.234	0.110	0.277	0.119	0.112	0.119
A16	0	11.943	10.278	6.137	7.236	6.095	15.275	10.581	14.068	12.731	7.445	8.226	8.957	7.432	9.427
A17		0	0.000	0.268	0.000	0.000	0.350	0.260	0.347	0.253	0.000	0.299	0.000	0.000	0.000
A18			0	0.123	0.298	0.298	0.338	0.120	0.120	0.104	0.301	0.068	0.298	0.298	0.298
A19				0	0.268	0.267	0.352	0.082	0.081	0.070	0.266	0.116	0.268	0.268	0.268
A20					0	0.000	0.356	0.261	0.267	0.251	0.000	0.297	0.000	0.000	0.000
A21						0	0.356	0.260	0.348	0.251	0.000	0.297	0.000	0.000	0.000
A22							0	0.347	0.098	0.332	0.349	0.323	0.356	0.348	0.356
A23								0	0.098	0.087	0.259	0.113	0.261	0.261	0.262
A24									0	0.076	0.266	0.120	0.268	0.265	0.267
A25										0	0.251	0.104	0.251	0.251	0.251
A26											0	0.298	0.000	0.000	0.000
A27												0	0.297	0.297	0.297
A28													0	0.000	0.000
A29														0	0.000
A30															0

Table 6: B-factor of the catalytic residues of the *Arthrobacter* β-mannanases

	1st catalytic residue		2nd catalytic residue	
Protein ID	Position	B-factor	Position	B-factor
MeMan5A	E177	-	E307	-
TriMan5A	E165	-	E275	-
CfMan26	E173	-	E280	-
A1	E231	24.15	E342	29.64
A2	E239	24.11	E350	25.59
A3	E172	26.59	E325	27.79
A4	E234	21.89	E345	28.55
A5	E233	21.67	E344	31.27
A6	E236	20.76	E347	30.02
A7	E239	23.85	E350	25.01
A8	E233	20.75	E344	24.60
A9	E267	21.20	E378	31.31
A10	E259	20.00	E370	25.57
A11	E209	24.10	E320	30.79
A12	E238	22.92	E349	30.65
A13	E238	25.00	E349	30.43
A14	E209	24.42	E320	30.71
A15	E227	24.46	E338	32.51
A16	D249	30.17	-	-
A17	E233	22.45	E344	31.01
A18	E232	23.97	E343	31.40
A19	E246	20.88	E357	30.43
A20	E237	21.61	E348	30.59
A21	E240	21.16	E351	31.58
A22	E236	21.86	E347	31.92
A23	E264	22.84	E375	32.65
A24	E244	21.02	E355	31.70
A25	E239	20.32	E350	32.37
A26	E235	20.35	E346	27.94
A27	E219	21.70	E330	30.52
A28	E246	21.86	E357	30.27
A29	E227	20.70	E338	32.39
A30	E238	22.84	E349	29.96

varied. This might be due to the presence of an additional domain (apart from its catalytic domain), which is the carbohydrate-binding domain (CBM) which functions to anchor substrates more effectively[32,33]. Interestingly, Fig. 1 showed that most of *Arthrobacter* β-mannanases (except for Strain A16 and A13) were in the distinct branches or nodes of the well-known β-mannanases (MeMan5A, TriMan5A and CfMan26A). This might suggest that the historical evolution of *Arthrobacter* β-mannanases are different from MeMan5A, TriMan5A and CfMan26A and possibly exhibit unique properties. Meanwhile, pI value of the *Arthrobacter* β-mannanases also varied which suggests different pH adaptation of these proteins. It was previously confirmed that the pI value of an enzyme is related to the pH optimum for their catalytic activity and plays an important role in the solubility of the enzyme[34]. The instability index values of the full-length and catalytic domain of *Arthrobacter* β-mannanases were found to be lower than 40 (Table 3). The index refers to the prediction of protein stability in the test tube, whereby the greater index reflects lower stability. In particular, a protein with the index of lower than 40 is considerably stable[19]. This suggests that *Arthrobacter* β-mannanases are generally stable in the test tube.

In addition, Table 3 indicated that the aliphatic index showed that the index of mesophilic *Arthrobacter* β-mannanase is considerably higher than that of psychrophilic one. This is plausible since psychrophilic proteins were characterized by lower thermal stability than its mesophilic counterparts[35]. It is interesting that the GRAVY index value of the mesophilic *Arthrobacter* β-mannanases were found to be higher than that of the psychrophilic group. This suggested that the mesophilic *Arthrobacter* β-mannanases is more hydrophobic than the psychrophilic group. To note, hydrophobic interaction was known to play important role in the thermal stability of protein. Therefore, thermo-stable proteins are usually characterized by higher GRAVY index and more hydrophobic residues than the thermo-labile

proteins[36,37]. Nevertheless, Table 3 indicated that compositions of hydrophobic residues between mesophilic and psychrophilic *Arthrobacter* β-mannanase were similar. Note that the composition only refers to the number of hydrophobic residues, regardless of the magnitude of their hydrophobicity. Accordingly, similar number of hydrophobic residues between these 2 groups does not necessarily imply that both are similarly hydrophobic. As the GRAVY index is obviously different, it is assumed that the psychrophilic *Arthrobacter* β-mannanase is dominated by less bulky hydrophobic residues which then leads to less hydrophobic than the mesophilic ones.

Overall features of amino acid composition of *Arthrobacter* β-mannanase indicated the domination of the hydrophobic residues (Fig. 4). Similarly, β-mannanase from alkaliphilic *Bacillus* sp. N16-5 was also reported to be dominated by hydrophobic residues[11]. Apart from the involvement of hydrophobic residues in structural stability, these residues might also be catalytically important for substrate binding and were often found in the substrate-binding pocket[38-40]. The domination of hydrophobic residues in *Arthrobacter* β-mannanase was followed by polar uncharged and charged residues. The uncharged residues were reported to be heavily involved in the solvation of the protein as the residues were mostly located on the surface of the protein[41]. On the other hand, hydrophilic residues are believed to play a role in the formation of any ionic interaction, hydrogen bond and the Van Der Waals interaction stabilizing the proteins.

Interestingly, while generally cold-adapted enzymes are characterized by lower charged residues[42,43], Table 3 indicated that charged residues of psychrophilic *Arthrobacter* β-mannanase were found to be slightly higher than the mesophilic ones (Table 3). Nevertheless, Gianese *et al.*[44] indicated that rather than the composition (number) of charged residues, their spatial distribution is more important to cold-adaptation strategy. Thermophilic enzymes tend to have more charged residues in their flexible regions in order to increase the stability by compensating the structural entropy. In addition, the ratios of positively and negatively charged residues were also reported to be the factors for cold-adaptation[45]. Nevertheless, Table 3 showed that both psychrophilic and mesophilic *Arthrobacter* β-mannanases showed lower positively charged residues compared to the negatively charged residues. This indicated that adjustments of charged residues might not be the main strategy of thermal adaptation for *Arthrobacter* β-mannanase. Alternatively, the structural distributions of charged residues not the number, are the main factors affecting the thermal adaptation of the enzyme. Nevertheless, further structural investigation on the distribution is needed to confirm this assumption.

Secondary structural analysis revealed that the full-length of psychrophilic *Arthrobacter* β-mannanase had a higher content of random coil as compared to the mesophilic one. This indicated that the full-length adopted a strategy of destabilizing some regions, particularly the coil, to adapt to the low temperature. The coil structure was known to be the flexible region in the protein structure and often determines protein stability. In some cases, the region is found to be disordered due to high flexibility[46]. Accordingly, cold-adapted enzymes often have a more flexible region as compared to the mesophilic or thermophilic counterparts. Further, the average helical structure content of psychrophilic *Arthrobacter* β-mannanase was considerably lower than the mesophilic one (Table 4, Fig. 5). This is believed to be associated with the structural stability as the longer helical structure is reported to be more stable than the shorter one[47]. It is interesting that the catalytic domain has comparable helical content (<1% differences) than the full-length, which suggested that the adaptation to low temperature by psychrophilic *Arthrobacter* β-mannanase is dictated by its full-length structure.

Furthermore, the fact that all 3D-models of psychrophilic and mesophilic *Arthrobacter* β-mannanase were similar (Fig. 6, Table 5) and indicated that the tertiary structure has no or little effect on the temperature adaptation of the enzyme. Rather, secondary and local structure arrangements as discussed above, play a more important role in the adaptation. Indeed, the B-factor of the second glutamic acid active site of the psychrophilic *Arthrobacter* β-mannanase is similar yet has a wider range compared to that of the mesophilic one (Fig. 7, Table 6). The B-factor reflects the fluctuation of atoms about their average positions which suggests that the protein with higher B-factor is considerably highly dynamic (flexible)[48]. Accordingly, the second glutamic acid active site of the psychrophilic *Arthrobacter* β-mannanase exhibited higher flexibility than that of the mesophilic one. It is known that the flexibility of the area around the catalytic pocket is one of the strategies of cold-adapted enzymes. Nevertheless, the high structural similarity of psychrophilic and mesophilic *Arthrobacter* β-mannanase and conservation of the catalytic sites reflected that the enzymes shared similar mechanisms. This also implied that structural adjustment for thermal adaptation might be independent from the catalytic mechanism, however, it may indirectly have affected the catalysis properties.

CONCLUSION

β-mannanases from various *Arthrobacter* strains were shown to have high genetic relatedness and share the catalytic sites which indicated that the enzymes might employ similar catalytic mechanism. Nevertheless, comparative analysis on these β-mannanases displayed a variation of the physio-chemical and structural properties of the enzymes. The variation is believed to be associated with the adaptation of mechanisms to their respective environments. In particular, cold adaptation of psychrophilic β-mannanases was achieved by a series of adjustments on the secondary structure formation, flexibility (B-factor) around the active sites as well amino acid composition (hydrophilic, particularly negatively charged, residues and proline residues).

SIGNIFICANCE STATEMENT

This study discovers the structural differences of psychrophilic and mesophilic *Arthrobacter* β-mannanase that can be beneficial for further studies and industrial application. This study will help the researcher to uncover the critical areas of structural regulation of β-mannanases in thermal adaptation that many researchers were not able to explore. Thus, a new theory on the mechanism by which *Arthrobacter* β-mannanases adapt to low temperature may be arrived at.

ACKNOWLEDGMENT

This study was supported by SBK0253-SG-2016 and GUG0105-1/2017 research grants.

REFERENCES

1. Chauhan, P.S., S.P. Tripathi, A.T. Sangamwar, N. Puri, P. Sharma and N. Gupta, 2015. Cloning, molecular modeling and docking analysis of alkali-thermostable β-mannanase from *Bacillus nealsonii* PN-11. Applied Microbiol. Biotechnol., 99: 8917-8925.
2. Malgas, S., S.J. van Dyk and B.I. Pletschke, 2015. β-Mannanase (Man26A) and α-galactosidase (Aga27A) synergism-a key factor for the hydrolysis of galactomannan substrates. Enzyme Microb. Technol., 70: 1-8.
3. Dhawan, S. and J. Kaur, 2007. Microbial mannanases: An overview of production and applications. Crit. Rev. Biotechnol., 27: 197-216.
4. Chauhan, P.S., N. Puri, P. Sharma and N. Gupta, 2012. Mannanases: Microbial sources, production, properties and potential biotechnological applications. Applied Microbiol. Biotechnol., 93: 1817-1830.
5. Conn, H.J. and I. Dimmick, 1947. Soil bacteria similar in morphology to *Mycobacterium* and *Corynebacterium*. J. Bacteriol., 54: 291-303.
6. Dsouza, M., M.W. Taylor, S.J. Turner and J. Aislabie, 2015. Genomic and phenotypic insights into the ecology of *Arthrobacter* from Antarctic soils. BMC Genomics, Vol. 16. 10.1186/s12864-015-1220-2.
7. Fredrickson, J.K., J.M. Zachara, D.L. Balkwill, D. Kennedy and S.M.W. Li *et al*., 2004. Geomicrobiology of high-level nuclear waste-contaminated vadose sediments at the Hanford Site, Washington State. Applied Environ. Microbiol., 70: 4230-4241.
8. Hanbo, Z., D. Changqun, S. Qiyong, R. Weimin and S. Tao *et al*., 2004. Genetic and physiological diversity of phylogenetically and geographically distinct groups of *Arthrobacter* isolated from lead-zinc mine tailings. FEMS Microbiol. Ecol., 49: 333-341.
9. Gounot, A.M., 1986. Psychrophilic and psychrotrophic microorganisms. Experientia, 42: 1192-1197.
10. Ratkowsky, D.A., J. Olley, T.A. McMeekin and A. Ball, 1982. Relationship between temperature and growth rate of bacterial cultures. J. Bacteriol., 149: 1-5.
11. Zhao, Y., Y. Zhang, Y. Cao, J. Qi and L. Mao *et al*., 2011. Structural analysis of alkaline β-mannanase from alkaliphilic *Bacillus* sp. N16-5: Implications for adaptation to alkaline conditions. PLoS ONE, Vol. 6. 10.1371/journal.pone.0014608.
12. Dos Santos, C.R., J.H. Paiva, A.N. Meza, J. Cota and T.M. Alvarez *et al*., 2012. Molecular insights into substrate specificity and thermal stability of a bacterial GH5-CBM27 endo-1,4-β-D-mannanase. J. Struct. Biol., 177: 469-476.
13. Lieberman, R.L., 2019. How does a protein's structure spell the difference between health and disease? Our journey to understand glaucoma-associated myocilin. PLoS Biol., Vol. 17. 10.1371/journal.pbio.3000237.
14. Gerlt, J.A. and P.C. Babbitt, 2000. Can sequence determine function? Genome Biol., Vol. 1. 10.1186/gb-2000-1-5-reviews0005.
15. Silvester, J., H.U.A. Lindang, L.P. Chin, L.T. Ying and C. Budiman, 2017. Structure and molecular dynamic regulation of FKBP35 from *Plasmodium knowlesi* by structural homology modeling and electron microscopy. J. Biol. Sci., 17: 369-380.
16. Zanghellini, A., L. Jiang, A.M. Wollacott, G. Cheng and J. Meiler *et al*., 2006. New algorithms and an *in silico* benchmark for computational enzyme design. Protein Sci., 15: 2785-2794.
17. Felsenstein, J., 2005. PHYLIP (phylogeny inference package) version 3.6. Department of Genome Sciences, University of Washington, Seattle, USA.
18. Gasteiger, E., C. Hoogland, A. Gattiker, S. Duvaud, M.R. Wilkins, R.D. Appel and A. Bairoch, 2005. Protein Identification and Analysis Tools on the ExPASy Server. In: The Proteomics Protocols Handbook, Walker, J.M. (Ed.). 1st Edn., Humana Press, New Jersey, USA., ISBN-13: 978-1588295934, pp: 571-607.

19. Guruprasad, K., B.V.B. Reddy and M.W. Pandit, 1990. Correlation between stability of a protein and its dipeptide composition: A novel approach for predicting *in vivo* stability of a protein from its primary sequence. Protein Eng. Des. Sel., 4: 155-161.
20. Ikai, A., 1980. Thermostability and aliphatic index of globular proteins. J. Biochem., 88: 1895-1898.
21. Kyte, J. and R.E. Doolittle, 1982. A simple method for displaying the hydropathic character of a protein. J. Mol. Biol., 157: 105-132.
22. McGuffin, L.J., K. Bryson and D.T. Jones, 2000. The PSIPRED protein structure prediction server. Bioinformatics, 16: 404-405.
23. Al-Shatnawi, M., M.O. Ahmad and M.N.S. Swamy, 2015. MSAIndelFR: A scheme for multiple protein sequence alignment using information on indel flanking regions. BMC Bioinform., Vol. 16. 10.1186/s12859-015-0826-3.
24. Tamura, K., G. Stecher, D. Peterson, A. Filipski and S. Kumar, 2013. MEGA6: Molecular evolutionary genetics analysis version 6.0. Mol. Biol. Evol., 30: 2725-2729.
25. Soderberg, O., M. Gullberg, M. Jarvius, K. Ridderstrale and K.J. Leuchowius *et al*., 2006. Direct observation of individual endogenous protein complexes *in situ* by proximity ligation. Nat. Methods, 3: 995-1000.
26. Le Nours, J., L. Anderson, D. Stoll, H. Stalbrand and L. Lo Leggio, 2005. The structure and characterization of a modular endo-β-1,4-mannanase from *Cellulomonas fimi*. Biochemistry, 44: 12700-12708.
27. Sabini, E., H. Schubert, G. Murshudov, K.S. Wilson, M. Siika-Aho and M. Penttila, 2000. The three-dimensional structure of a *Trichoderma reesei β*-mannanase from glycoside hydrolase family 5. Acta Crystallogr. Sect. D: Biol. Crystallogr., 56: 3-13.
28. Waterhouse, A., M. Bertoni, S. Bienert, G. Studer and G. Tauriello *et al*., 2018. SWISS-MODEL: Homology modelling of protein structures and complexes. Nucleic Acids Res., 46: W296-W303.
29. Kelley, L.A., S. Mezulis, C.M. Yates, M.N. Wass and M.J. Sternberg, 2015. The Phyre2 web portal for protein modeling, prediction and analysis. Nat. Protocols, 10: 845-858.
30. Eisenberg, D., R. Luthy and J.U. Bowie, 1997. VERIFY3D: Assessment of protein models with three-dimensional profiles. Methods Enzymol., 277: 396-404.
31. Yang, J., Y. Wang and Y. Zhang, 2016. ResQ: An approach to unified estimation of *B*-factor and residue-specific error in protein structure prediction. J. Mol. Biol., 428: 693-701.
32. Abbott, D.W., J.M. Eirin-Lopez and A.B. Boraston, 2008. Insight into ligand diversity and novel biological roles for family 32 carbohydrate-binding modules. Mol. Biol. Evol., 25: 155-167.
33. Boraston, A.B., T.J. Revett, C.M. Boraston, D. Nurizzo and G.J. Davies, 2003. Structural and thermodynamic dissection of specific mannan recognition by a carbohydrate binding module, *TmCBM27*. Structure, 11: 665-675.
34. Talley, K. and E. Alexov, 2010. On the pH-optimum of activity and stability of proteins. Proteins: Struct. Funct. Bioinform., 78: 2699-2706.
35. Idicula-Thomas, S. and P.V. Balaji, 2005. Understanding the relationship between the primary structure of proteins and its propensity to be soluble on overexpression in *Escherichia coli*. Protein Sci., 14: 582-592.
36. Kulakova, L., A. Galkin, T. Kurihara, T. Yoshimura and N. Esaki, 1999. Cold-active serine alkaline protease from the psychrotrophic bacterium *Shewanella* strain Ac10: Gene cloning and enzyme purification and characterization. Applied Environ. Microbiol., 65: 611-617.
37. Metpally, R.P.R. and B.V.B. Reddy, 2009. Comparative proteome analysis of psychrophilic *versus* mesophilic bacterial species: Insights into the molecular basis of cold adaptation of proteins. BMC Genomics, Vol. 10. 10.1186/1471-2164-10-11.
38. Henrissat, B., 1991. A classification of glycosyl hydrolases based on amino acid Sequence similarities. Biochem. J., 280: 309-316.
39. Hogg, D., E.J. Woo, D.N. Bolam, V.A. McKie, H.J. Gilbert and R.W. Pickersgill, 2001. Crystal structure of mannanase 26A from *Pseudomonas cellulosa* and analysis of residues involved in substrate binding. J. Biol. Chem., 276: 31186-31192.
40. McCleary, B.V. and N.K. Matheson, 1983. Action patterns and substrate-binding requirements of β-D-mannanase with mannosaccharides and mannan-type polysaccharides. Carbohydr. Res., 119: 191-219.
41. Green, S.M., A.K. Meeker and D. Shortle, 1992. Contributions of the polar, uncharged amino acids to the stability of staphylococcal nuclease: Evidence for mutational effects on the free energy of the denatured state. Biochemistry, 31: 5717-5728.
42. Michetti, D., B.O. Brandsdal, D. Bon, G.V. Isaksen, M. Tiberti and E. Papaleo, 2017. A comparative study of cold-and warm-adapted Endonucleases A using sequence analyses and molecular dynamics simulations. PLoS ONE, Vol. 12. 10.1371/journal.pone.0169586.
43. Das, R. and M. Gerstein, 2000. The stability of thermophilic proteins: A study based on comprehensive genome comparison. Funct. Integr. Genomics, 1: 76-88.

44. Gianese, G., P. Argos and S. Pascarella, 2001. Structural adaptation of enzymes to low temperatures. Protein Eng., 14: 141-148.
45. Siddiqui, K.S. and R. Cavicchioli, 2006. Cold-adapted enzymes. Annu. Rev. Biochem., 75: 403-433.
46. Iakoucheva, L.M. and A.K. Dunker, 2003. Order, disorder and flexibility: Prediction from protein sequence. Structure, 11: 1316-1317.
47. Stanger, H.E., A.S. Faisal, J.F. Espinosa, I. Giriat, T. Muir and S.H. Gellman, 2001. Length-dependent stability and strand length limits in antiparallel β-sheet secondary structure. Proc. Natl. Acad. Sci. USA., 98: 12015-12020.
48. Wang, P., Y. Qu and J. Zhou, 2009. Biodegradation of mixed phenolic compounds under high salt conditions and salinity fluctuations by *Arthrobacter* sp. W1. Applied Biochem. Biotechnol., 159: 623-633.